Complement C3-dependent glutamatergic synapse elimination in the developing hippocampus is region- and synapse-specific

Authors: Eric W. Salter[1,2], Gang Lei[2], Sun-Lim Choi[2], Liam T. Ralph[1,2], Lijia Zhang[2], Fuzi Jin[2], Ashish Kadia[2], Junhui Wang[2], John Georgiou[2] and Graham L. Collingridge[1,2,3,4,5].

Affiliations:

1. Department of Physiology, University of Toronto, Toronto, Ontario, M5S 1A8, Canada

2. Lunenfeld-Tanenbaum Research Institute, Mount Sinai Hospital, Sinai Health System, Toronto, Ontario, M5G 1X5, Canada

3. Glutamate Research Group, School of Physiology, Pharmacology and Neuroscience, University of Bristol, BS8 1TD, United Kingdom

4. TANZ Centre for Research in Neurodegenerative Diseases, University of Toronto, Toronto, Ontario, M5S 1A8, Canada

5. Corresponding author. Email: Collingridge@lunenfeld.ca

Summary

The complement cascade is an innate immune pathway that, in addition to host defense against pathogens, actively maintains tissue homeostasis. Complement is necessary for synaptic pruning during development and drives aberrant synapse loss in a number of neurodegenerative disorders that affect the hippocampus. However, the physiological function of complement in hippocampal synapse development is unknown. To address this, we investigated $C3^{-/-}$ mice at P16-18. We found that $VGLUT2^+$ synapses were increased in the CA1 stratum lacunosum moleculare (SLM) and dentate gyrus molecular layer (DGML) of $C3^{-/-}$ mice compared to wildtype. Conversely, $VGLUT1^+$ synapses, inhibitory synapses and myelin were not affected in the CA1 stratum radiatum (SR), SLM or DGML of $C3^{-/-}$ mice. Finally, we found that there was a decrease in microglial phagocytic activity only in $VGLUT2^+$ regions and this correlated with the amount of $VGLUT2^+$ synapses. Our study elucidates a role of the complement cascade in regulating hippocampus synapse number with exceptional specificity for VGLUT2-containing synapses during development.

Introduction

The complement cascade is an innate immune pathway originally discovered for its role in opsonizing and eliminating foreign pathogens. In addition to host defense, complement is instrumental in normal physiology to maintain tissue homeostasis (Ricklin et al., 2010). A fundamental process of central nervous system (CNS) development is synaptic pruning. Initially, excess synapses are generated and neuronal activity dictates which synapses are kept to properly wire the brain (Hua and Smith, 2004; Katz and Shatz, 1996). The complement cascade has been found to be a critical pathway in this developmental synaptic pruning (Schafer et al., 2012; Stevens et al., 2007). Additionally, accumulating evidence indicates that aberrant activation of the complement cascade is a central driver of pathology in multiple neurological disorders including Alzheimer's disease (Bie et al., 2019; Dejanovic et al., 2018; Hammond et al., 2020; Hong et al., 2016; Litvinchuk et al., 2018; Roy et al., 2020; Shi et al., 2017; Wu et al., 2019), age-related cognitive decline (Shi et al., 2015; Stephan et al., 2013), multiple sclerosis (Hammond et al., 2020; Watkins et al., 2016; Werneburg et al., 2020) and schizophrenia (Comer et al., 2020; Sekar et al., 2016; Sellgren et al., 2019). A prevailing hypothesis is that pathological reactivation of complement-dependent synaptic pruning in adulthood is a common mechanism underlying these disorders, leading to synapse loss and neurodegeneration (Chung et al., 2015; Salter and Stevens, 2017; Stephan et al., 2012). Thus, a detailed understanding of the mechanisms of complement-dependent synaptic pruning during development will provide crucial insight into multiple brain disorders.

Initiation of the classical arm of the complement cascade begins with C1q, which binds to damage/pathogen associated molecular patterns (DAMPs/PAMPs) on the target

3

structure, such as a synapse. Upon C1q binding, a series of proteolytic reactions occur leading to the generation of the C3 convertase, which cleaves C3 into C3a and C3b fragments. C3b covalently binds to the target structure and is further cleaved into iC3b, which sets the 'eat me' signal, referred to as opsonization. Binding of iC3b to CR3 (comprised of subunits CD11b and CD18) triggers phagocytosis (Ricklin et al., 2010). In the healthy CNS, microglia are the only cells to express C1q (Fonseca et al., 2017) and CR3, placing microglia as central effectors of physiological complement function in the brain. Microglia are the resident immune cells in the CNS derived from yolk-sac progenitors, migrating into the CNS at embryonic day (E) 8.5 (Ginhoux et al., 2010; Perdiguero et al., 2015) to constantly monitor the brain parenchyma (Davalos et al., 2005; Nimmerjahn et al., 2005). Stevens and colleagues (2007) identified that complement was necessary for synaptic pruning in the developing visual system. Genetic deletion of either C1q or C3 prevented segregation of synaptic inputs into eye-specific regions in the dorsolateral geniculate nucleus (dLGN). Furthermore, microglia had reduced phagocytosis of synapses in the dLGN in C3- or CR3-deficient mice (Schafer et al., 2012). Subsequently, complement has been found to mediate developmental synaptic pruning in other regions of the CNS including excitatory synapses in the olfactory bulb (Lehmann et al., 2018) and spinal cord (Vukojicic et al., 2019) as well as dopamine receptors in the nucleus accumbens (Kopec et al., 2018).

The hippocampus is a major brain region where it is unclear whether complement-dependent pruning occurs during development. This region is a central structure for learning and memory in the brain (Andersen et al., 2006) and is affected in the majority of disorders that are driven by the complement cascade. Therefore, determining the role

of complement in hippocampus development has important implications for understanding how complement shapes synapses in higher-order cognitive brain regions and how this process goes awry in disease.

Within the hippocampus, there are two principal vesicular glutamate transporter (VGLUT) isoforms, VGLUT1 and VGLUT2, which are segregated to distinct regions and synaptic circuits within the hippocampus. The distal CA1 stratum lacunosum moleculare (CA1 SLM) and the dentate gyrus molecular layer (DGML) receive extra-hippocampal inputs from the entorhinal cortex. In these regions VGLUT2 is the main synaptic isoform. Conversely, within the CA1 stratum radiatum (SR), which receives intra-hippocampal inputs from CA3, VGLUT1 predominates (see Figure 1A, B). Thus, excitatory synapses in the hippocampus can be categorized by their localization and the VGLUT isoform expressed. Our study elucidates the role of the complement cascade in hippocampal synapse development by identifying that complement C3-dependent pruning occurs only at VGLUT2-positive ($^+$) synapses in the CA1 SLM and the DGML. Conversely, neither VGLUT1$^+$ synapses, inhibitory synapses or myelin protein are affected in the CA1 SR, SLM and DGML of C3$^{-/-}$ mice. These data demonstrate that in the developing hippocampus, complement regulates specifically the number of VGLUT2$^+$ synapses.

Results

Developmental trajectory of VGLUTs in hippocampus development

We first characterized the changes to VGLUT1 and VGLUT2 protein levels during postnatal development in the hippocampus. We observed that while VGLUT1 increases nearly monotonically with postnatal age, VGLUT2 peaks at postnatal day (P)5 and decreases thereafter (Figure 1B), similar to previous findings (Berry et al., 2012; Boulland

et al., 2004). The changes in VGLUT2 qualitatively reflect a typical pruning curve, in which supernumerary synapses are generated and subsequently refined (e.g. Huttenlocher, 1979; Petanjek et al., 2011). Additionally, it has been found that the initiating protein of the classical arm of the complement cascade, C1q, localizes preferentially to the DGML and CA1 SLM (Stephan et al., 2013), where VGLUT2^{+} synapses are found in the hippocampus. Therefore, we hypothesized that there exists a developmental complement-mediated pruning program in the hippocampus that occurs specifically at VGLUT2^{+} synapses within the CA1 SLM and DGML.

VGLUT2^{+} synapses are increased in C3$^{-/-}$ mice

To examine the role of the complement cascade in hippocampal synaptic refinement during development, we used C3 knockout mice (C3$^{-/-}$; Wessels et al., 1995), which lack the protein necessary for opsonization by the complement cascade. To investigate synapses in a region- and VGLUT isoform specific-manner, we performed immunohistofluorescence on PFA-fixed brains from C3$^{-/-}$ mice and their wildtype (WT) littermates at P16-18. We began by investigating VGLUT2^{+} synapses in the CA1 SLM and DGML. Consistent with our hypothesis, C3$^{-/-}$ mice had a significantly higher volume of VGLUT2 signal in CA1 SLM compared to WT littermates (Figure 1C, D). Similarly, in the DGML there was a significant increase of VGLUT2 in C3$^{-/-}$ mice compared to WT littermates (Figure 1E, F). To determine whether this increase in presynaptic VGLUT2 translated to an increase in putative synapses, we examined the co-localization between VGLUT2 and Homer1, a postsynaptic protein (Sheng and Kim, 2011). We found a significant increase in the volume of co-localization between VGLUT2 and Homer1 in

6

C3$^{-/-}$ mice compared to WT littermates in both the CA1 SLM (Figure 1C, D) and the DGML (Figure 1E, F). Interestingly, we found that the volume of postsynaptic Homer1 was not increased in the CA1 SLM, however there was a significant increase in the DGML (Figure 1C-F). These data indicate that complement C3 targets VGLUT2-containing synapses in both the CA1 SLM and DGML. However, an increase of Homer1-containing postsynaptic elements is specific to the DGML. As such, the identity of the postsynaptic neuron is a critical factor for complement-dependent regulation of the post-synapse.

C3$^{-/-}$ mice do not have altered VGLUT1$^+$ synapses

We next investigated VGLUT1$^+$ synapses to determine whether all types of excitatory pre-synapses are increased in C3-lacking mice. In the CA1 SR, we found there was no difference in the volume of VGLUT1 signal between WT and C3$^{-/-}$ mice (Figure 2A, B). Further, there was no increase in Homer1 or VGLUT1 and Homer1 co-localized volume within the CA1 SR of C3$^{-/-}$ mice compared to WT littermates (Figure 2A, B). These data indicate that the number of excitatory synapses in the CA1 SR is not regulated by a complement C3-dependent mechanism.

Although VGLUT2 is the main VGLUT isoform in the CA1 SLM and DGML, there are also VGLUT1$^+$ synapses in both of these regions. Therefore, we sought to determine if the increase of synapses in C3$^{-/-}$ mice is dependent on hippocampus sub-region (CA1 SR vs. CA1 SLM and DGML) or VGLUT type (VGLUT1 vs. VGLUT2). We found there was no significant difference in VGLUT1 volume in the CA1 SLM (Figure 2C, D) or the DGML (Figure 2E, F) between WT and C3$^{-/-}$ mice. Further, VGLUT1 and Homer1 co-

localized volume was not increased in C3$^{-/-}$ mice compared to WT in either the CA1 SLM (Figure 2C, D) or the DGML (Figure 2E, F). Collectively, these data demonstrate that complement-dependent regulation of synapses in the developing hippocampus is determined by both VGLUT type and region.

Inhibitory synapses and myelin are not affected in C3$^{-/-}$ mice

Next, we sought to determine whether regulation of synapse number by C3 also occurs at inhibitory synapses during hippocampus development. We imaged the inhibitory presynaptic bouton marker vesicular GABA transporter (VGAT) across the CA1 SR, CA1 SLM and DGML. We did not find any significant difference between WT and C3$^{-/-}$ mice in the volume of VGAT across any of these three hippocampal regions (Figure 3A, B). We also evaluated whether there was an increase in a myelin marker in C3$^{-/-}$ mice as it has been recently found that microglia phagocytose oligodendrocytes and myelin sheaths during development (Hughes et al., 2019; Li et al., 2019). To mark oligodendrocytes and myelin sheaths, we stained for myelin basic protein (MBP). We found no difference in MBP volume in either the CA1 SR, CA1 SLM or DGML in C3$^{-/-}$ mice compared to WT (Figure 3C, D). Collectively, our data demonstrates that VGLUT2^{+} synapses in the developing hippocampus are selected for regulation by complement C3.

Region-specific reduction in microglial phagocytic activity in C3$^{-/-}$ mice

The increase of VGLUT2^{+} synapses in C3$^{-/-}$ mice suggested there was a pruning deficit due to reduced synapse phagocytosis by microglia. Synaptic material which has been phagocytosed by microglia has been found to localize to CD68, a marker of

8

microglial lysosomes (Schafer et al., 2012; Schafer et al., 2014; Werneburg et al., 2020). Therefore, we examined if there was a corresponding reduction in microglial phagocytosis within regions with increased VGLUT2$^+$ synapses in C3$^{-/-}$ mice. We normalized the volume of CD68 to Iba1 (Filipello, Morini et al., 2018), which we refer to as the 'phagocytic index', to quantify the amount of ongoing phagocytic activity per unit of microglia. In the CA1 SR, there was no difference in the phagocytic index between WT and C3$^{-/-}$ mice (Figure 4A, B). This aligns with our previous data in the CA1 SR which found no difference in VGLUT1$^+$ and VGAT synapses or MBP (Figure 2, 3). Furthermore, there was no significant correlation between VGLUT1 and Homer1 co-localized volume and phagocytic index in the CA1 SR (Figure 4C). However, there was a significant reduction of the phagocytic index in C3$^{-/-}$ mice compared to WT in both the CA1 SLM (Figure 4D, E) and the DGML (Figure 4G, H). Also, there was a significant negative correlation between phagocytic index and VGLUT2 and Homer1 co-localization, but not VGLUT1 and Homer1 co-localization, in the CA1 SLM (Figure 4F) and DGML (Figure 4I). Overall, the corresponding increase of VGLUT2$^+$ synapses and decrease in phagocytic index in the CA1 SLM and DGML suggests that C3 mediates specifically microglial engulfment of VGLUT2$^+$ synapses in the developing hippocampus.

Discussion

Our study defines a role for the complement cascade in physiological synaptic development in the hippocampus. We demonstrate that in C3$^{-/-}$ mice, there is an increase in VGLUT2$^+$ synapses in the CA1 SLM and DGML regions of the hippocampus, whilst VGLUT1$^+$ synapses in the CA1 SR, CA1 SLM and DGML are unaffected. Moreover,

9

inhibitory synapses and myelin are not changed in $C3^{-/-}$ mice compared to WT. There is a decrease in microglial phagocytic activity only in the CA1 SLM and DGML, but not CA1 SR. Finally, the decreased phagocytic index correlated negatively with the amount of VGLUT2$^+$, but not VGLUT1$^+$ synapses. Given the known role of C3 and complement in synapse phagocytosis, we conclude that C3 targets specifically VGLUT2$^+$ but not VGLUT1$^+$ synapses in the hippocampus for elimination by microglia.

One of the main questions arising from our findings is: what directs complement-mediated synapse elimination to VGLUT2$^+$ synapses compared to VGLUT1$^+$ synapses? The entorhinal cortex (EC) provides the primary input to the CA1 SLM and DGML (Figure 1A). Expression of both VGLUT1 and VGLUT2 mRNA has been found in the EC (Fremeau Jr et al., 2001; Fremeau Jr et al., 2004; Wouterlood et al., 2008; Yekhlef et al., 2017). Therefore, one possibility is that VGLUT1 and VGLUT2 expressing cells which project to the hippocampus (i.e. such as from the EC) form distinct populations of neurons whose function and/or transcriptome differs such that only the VGLUT2-expressing cells have synapses susceptible to complement-dependent elimination. Conceptually, the reason for this difference in susceptibility could be due to either expression of protective signals, and/or a lack of complement-activating signals in VGLUT1-expressing cells. CD47 is a negative regulator of phagocytosis and has been found to serve as a 'don't eat me signal' to protect synapses in the dLGN from microglial engulfment through binding to microglial SIRPα (Lehrman et al., 2018). Additionally, regulators of complement activation (RCA) are a network of proteins that control complement cascade activation (Kim and Song, 2006; Ricklin et al., 2010). Thus, VGLUT1-expressing cells may preferentially

10

express one, or a number of these proteins to prevent complement activation and phagocytosis. Neural activity has been found to regulate microglia motility and interactions with neurons (Dissing-Olesen et al., 2014; Eyo et al., 2018; Liu et al., 2019) and is critical for complement-mediated pruning in the dLGN (Schafer et al., 2012). As such, it is also conceivable that VGLUT1- and VGLUT2-expressing neurons may have distinct firing patterns and synaptic plasticity mechanisms that promote complement activation and/or downregulate 'don't eat me signals' only at VGLUT2$^+$ synapses. A detailed analysis of transcriptional and functional differences between VGLUT1 and VGLUT2 expressing neurons which project to the hippocampus can provide important insight into the mechanisms and regulation of complement C3-dependent synapse pruning.

Understanding why certain synapses are protected from complement-mediated pruning may inform us about diseases driven by complement-dependent synapse loss, such as Alzheimer's disease (Dejanovic et al., 2018; Hong et al., 2016; Litvinchuk et al., 2018; Roy et al., 2020; Shi et al., 2017; Wu et al., 2019) and multiple sclerosis (Hammond et al., 2020; Werneburg et al., 2020). It has been proposed that complement-dependent synapse loss in disease is due to pathological re-activation of developmental pruning programs (Chung et al., 2015; Salter and Stevens, 2017; Stephan et al., 2012). Studies have found that the entorhinal cortex is one of the first regions affected in Alzheimer's disease (Braak et al., 2006; Gómez-Isla et al., 1996; Huijbers et al. 2014; Khan et al., 2014; Small et al., 2011; Thal et al., 2002; Yang et al., 2018). However, both pre- and post-synaptic elements in the CA1 SR (amongst other regions) are aberrantly eliminated

in Alzheimer's disease and multiple sclerosis in a complement-dependent manner (Bie et al., 2019; Dejanovic et al., 2018; Hammond et al., 2020; Hong et al., 2016; Litvinchuk et al., 2018; Roy et al., 2020; Wu et al., 2019) which we found to not occur in development. Additionally, it has been found that LPS combined with hypoxia can produce CR3-dependent synaptic depression in the CA1 SR (Zhang et al., 2014). Therefore, susceptibility to pathological complement-mediated synapse loss in disease is not simply a reflection of developmental synapse pruning programs. We propose it may instead be the result of inappropriate re-activation of developmental pathways in conjunction with loss of endogenous mechanisms that normally protect synapses from complement-mediated pruning.

In both the CA1 SLM and DGML, the pre-synaptic component of VGLUT2^{+} synapses were found to be targeted by complement C3 for elimination. This pre-synaptic phenotype mirrors what has been found in the dLGN (Schafer et al., 2012; Stevens et al., 2007). Also, a study of cortical synaptosomes found that C1q preferentially localizes to the pre-synapse (Györffy et al., 2018). Thus, targeting of pre-synapse for pruning by complement appears to be a common feature across multiple brain regions.

A recent study found that in the adult hippocampus, the complement cascade is necessary for forgetting (Wang et al., 2020). Expression of the C3 convertase inhibitor CD55 in dentate gyrus engram cells prevented forgetting of contextual fear memory, increased spine density and reduced microglial phagocytosis of engram cell spines. While the role of pre-synaptic elimination was not investigated, post-synaptic complement-

12

dependent pruning in the dentate gyrus may be a shared feature of developmental and learning-induced synapse pruning. Others have found that forgetting of contextual fear memory is substantially higher in P17 mice compared to adults, which has been termed infantile amnesia (Akers et al., 2014; Guskjolen et al., 2018). As this age coincides with the age of mice used in the current study, developmental complement-mediated pruning in the hippocampus may be part of the mechanism for infantile amnesia, and future studies will seek to address this.

Our findings are in line with previous studies which found that C3$^{-/-}$ mice have no difference in CA1 SR dendritic spine number at P17-30 (Perez-Alcazer et al., 2014) and that trogocytosis of excitatory pre-synapses in the CA1 SR is independent of CR3 (Weinhard et al., 2018). While collectively, these results demonstrate that a complement-dependent synapse elimination mechanism does not target synapses in the CA1 SR of the developing hippocampus, others have found that different microglial receptors mediate synapse elimination in this region. Deletion of the fractalkine receptor CX3CR1 was found to increase the number of dendritic spines in the CA1 SR (Paolicelli et al., 2011) as well as control pre-synaptic release probability (Basilico et al., 2019). Additionally, the innate immune receptor triggering receptor expressed on myeloid cells 2 (TREM2) has been found to contribute to synaptic pruning in the CA1 SR (Filipello, Morini et al., 2018). A series of recent publications have highlighted that synaptic exposure of phosphatidylserine (PS) is a central component of synaptic pruning. Scott-Hewitt, Perrucci et al. (2020) demonstrated that PS^{+} synapses in the CA1 SR were engulfed by microglia between P10-P18. Experiments in hippocampal cultures indicated

13

this is through binding to TREM2, which is known to bind to PS (Wang et al., 2015). Li et al. (2020) found that a separate microglial receptor, GPR56 also binds to PS. Knockout of GPR56 in microglia increased synapses in the CA1 SLM but not the CA1 SR. In conjunction with our findings, this suggests that TREM2-PS binding is selective for CA1 SR synapses while GPR56-PS interactions and complement C3 mediate CA1 SLM synapse elimination. Finally, Park et al. (2020) found that the PS receptor MERTK is important for elimination of inhibitory post-synapses in CA1, and the exposure of PS is controlled by CDC50A. In agreement with our results, they found C3$^{-/-}$ mice did not have altered numbers of inhibitory synapses. Thus, an emerging concept is that not all synapse phagocytosis events are the same in the hippocampus. This also suggests that there may be microglia subtype diversity within the hippocampus itself during development. Interestingly, a recent single-cell transcriptomic study of the developing human hippocampus found that microglia were divided into 11 sub-clusters (Zhong et al., 2020), demonstrating that hippocampal microglia are not uniform during human development. Therefore, microglial subpopulations with diverse 'appetites' for different types of synapses may be a conserved feature of microglial physiology in humans. Why this diversity exists is a fundamental question of microglia-synapse biology.

Our findings identify a role for complement C3 in hippocampal synapse development. We find that synapse elimination via complement is not a ubiquitous feature of all hippocampal synapses, instead exhibiting remarkable selectivity for VGLUT2^{+} synapses within the CA1 SLM and DGML. Understanding the features of synaptic function that drive this selectivity will provide important insights into the physiology of

14

complement-synapse interactions during development as well as how these processes go awry in a number of diseases. Our study further reveals that the developing hippocampus is an ideal brain region to study synapse-specific pruning via the complement cascade.

Methods

Animals

All experiments and procedures were approved by The Centre for Phenogenomics (TCP) animal care committee and conformed to the Canadian Council on Animal Care (CCAC) guidelines. Homozygous $C3^{-/-}$ mice (B6;129S4-C3^{tm1Crr}/J; stock no. 003641) were purchased from Jackson Laboratories and bred with our C57BL/6J colony. In all experiments, male homozygous knockout and wildtype littermate offspring from heterozygote-heterozygote crosses were used. Mice were allowed *ad libitum* access to food and water, and were maintained on a 12:12 hour light:dark schedule (lights on at 7:00 AM).

Brain fixation

All $C3^{-/-}$ mice and WT littermates were dissected with experimenter blinded to genotype. Brains were extracted, the frontal lobe and cerebellum were removed, and then were immersion fixed in 10 mL of cold (4°C), 4% PFA D-PBS prepared fresh from 16 % stock (EM Sciences, Cat no. 15710) and fixed for 18 hours at 4°C. Subsequently, brains were washed three times in D-PBS and then dehydrated in 20 mL of cold (4°C), 30 % sucrose D-PBS (w/v), and kept at 4°C for 48-72 hours. Finally, brains were embedded in OCT

15

(Tissue Tek, Cat no. 4583) or Tissue freezing medium (EM Sciences, Cat no. 72592), flash frozen on liquid nitrogen and stored at -80°C until sectioning.

Immunohistofluorescence

Embedded brains were cryosectioned coronally at 25 µm and mounted onto charged slides (ASSURE). Sections were stored at -80°C until staining. Sections were warmed to room temperature and washed 3 times in D-PBS to remove sectioning medium. Next, sections were blocked and permeabilized in 0.1% Triton X-100 D-PBS with 10 or 20% (for synapse markers and MBP or Iba1 and CD68, respectively) normal donkey serum (NDS; Jackson ImmunoResearch, cat. no. 017-000-001) for 1 hour at room temperature on a horizontal shaker. Then, sections were stained with primary antibodies in 0.1% Tween-20, 1% NDS, D-PBS at 4°C for 48 hours on a horizontal shaker. Primary antibodies were as follows: Guniea pig anti-VGLUT1 (1:1000, Millipore AB5905); Guinea pig anti-VGLUT2 (1:500, Synaptic Systems, 135 404); Rabbit anti-Homer1 (1:500, Synaptic Systems, 160 003); Rabbit anti-Iba1 (1:500, Wako, 019-19741); Rabbit anti-VGAT (1:500, Synaptic Systems, 131 003); Rat anti-CD68 (1:250, BioRad, MCA1957); Rat anti-MBP (1:250, Millipore MAB386). Sections were then rinsed four times in D-PBS and then stained with appropriate fluorophore-conjugated (Alexa 488, Cy3 or Cy5) donkey secondary antibodies from Jackson ImmunoResearch (1:500) and DAPI (Sigma-Aldrich, cat. no. D8417) in 0.1% Tween-20, 1% NDS, D-PBS for four hours at room temperature. Sections were then rinsed four times in D-PBS and mounted with 60 µL of ProLong Glass (Invitrogen, cat. no. P36980) and no. 1.5 high precision coverslips (Thorlabs, cat. no. CG15KH1). Mounted sections were kept at room temperature in the

16

dark for 24 hours to allow the mounting medium to cure (as per manufacturer instructions) and subsequently stored at 4°C in the dark until imaging.

Confocal imaging and analysis

Sections were imaged using a Nikon A1R HD25 confocal microscope. All images were acquired using a 60x oil objective (NA = 1.4) and 2x zoom at 1024 x 1024 pixels. Laser power and detector gain was kept constant for each imaging cohort. For synapse marker and MBP imaging, 4 µm z-stacks were acquired (z-step = 0.25 µm), while 12 or 15 µm z-stacks (z-step = 0.33 µm) were collected for Iba1/CD68 staining. For each hippocampus region imaged, 2 fields of view (FOVs) per section were acquired, and 2-3 sections per animal were imaged. Images were analyzed using Nikon NIS Elements. All imaging and analysis were performed blinded to genotype. All images within a cohort were subjected to identical image pre-processing (median filter, rolling ball subtraction) and thresholding steps. Following acquisition, the threshold was set manually using a subset of images capturing the full range of intensities and gave a value of 0 for secondary only controls. The amount of signal above threshold was quantified in the 3-D stack, yielding the volume of signal. For co-localization analysis, the binarized channels were combined using the Boolean 'AND' function, similar to previous studies (Cheadle et al., 2018; Filipello, Morini et al., 2018; Li et al., 2020; Litvinchuk et al., 2018; Lui et al., 2016; Scott-Hewitt et al., 2020; Vasek et al., 2016 Werneburg et al., 2020). Each measure was averaged across FOVs and slides for each animal and normalized to the WT mean.

Western Blotting

17

Hippocampi from WT C57BL/6J mice were isolated in ice-cold, oxygenated ACSF (in mM: 124 NaCl, 26 NaHCO$_3$, 3 KCL, 2 CaCl$_2$, 1 MgCl$_2$, 10 glucose) and snap frozen in liquid nitrogen then stored at -80°C. Subcellular fractionation to isolate the synaptosome was based on Hallett et al., 2008. Briefly, tissue was homogenized using a Dounce homogenizer in TEVP buffer (pH 7.4, 320 mM sucrose) and centrifuged at 800 x g for 10 min (all centrifugation was done at 4 ^{o}C). After removal of the supernatant, the pellet was resuspended in TEVP buffer and centrifuged for 15 min at 9,200 x g. The supernatant was again removed, and the remaining pellet was resuspended in TEVP buffer containing 35.6 mM sucrose and centrifuged for 20 min at 25,000 x g. Finally, the supernatant was again removed, and the remaining pellet was resuspended in TEVP buffer; this fraction is known as the LP1 fraction containing the synaptosome. Subsequently, the LP1 was run on an 8% SDS-polyacrylamide gel (10 μg/lane), and proteins were transferred onto a PVDF membrane. In all blots, 5% non-fat dairy milk was used for blocking. Membranes were incubated overnight at 4 ^{o}C in guinea pig anti-VGLUT1 (1:1000, Millipore AB5905) or guinea pig anti-VGLUT2 (1:8000, Millipore AB2251I) and incubated in secondary antibody (1:10,000; goat anti-guinea pig HRP-conjugated) for 2 hours at room temperature. Images were acquired on a Bio-Rad ChemiDoc.

Statistics

All data was graphed using GraphPad Prism 8. Unpaired two-tailed t-tests and Pearson correlation tests were performed using GraphPad Prism 8, and the p values are reported in the corresponding figure legend. All data is presented as mean ± SEM, and N values reflect the number of animals.
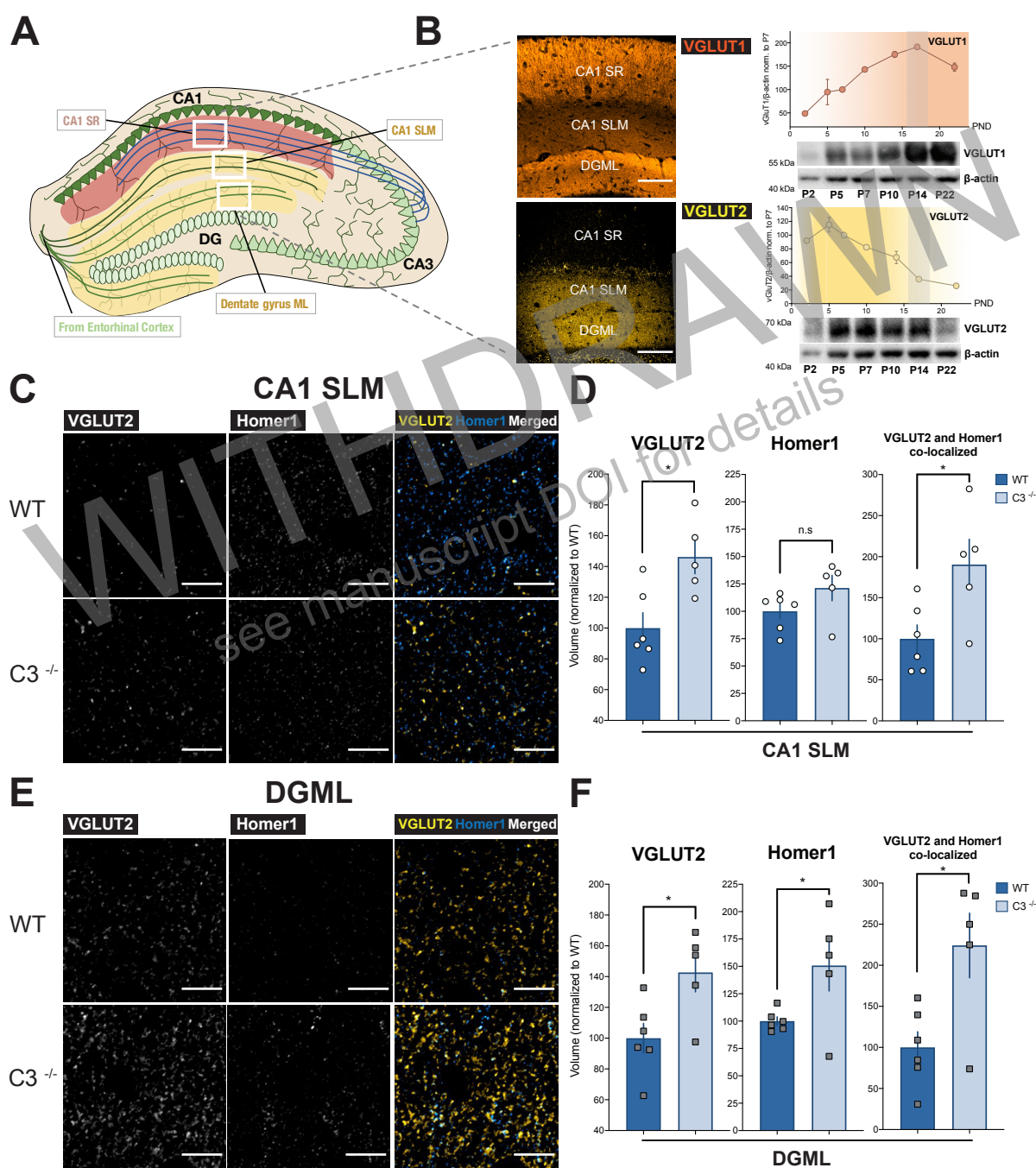
18

Figures

Figure 1. *Increased VGLUT2+ synapses in complement C3-/- mice.* **A** Schematic of hippocampal synaptic circuits investigated. White boxes indicate regions analyzed. **B**

Example maximum intensity projection (MIP) images of VGLUT1 and VGLUT2 distribution (left), and developmental time course of VGLUT1 and VGLUT2 protein levels in hippocampal LP1 fraction assayed by western blot (right), N = 2. Shaded grey region indicates age range used for IHF experiments. Scale bars, 100 μm. **C** Representative single plane confocal images of VGLUT2, Homer1 and co-localized VGLUT2 and Homer1 in the CA1 SLM of WT and C3$^{-/-}$ mice. Scale bars, 10 μm. **D** Quantification of VGLUT2 (*left*), Homer1 (*middle*) and VGLUT2 and Homer1 co-localized volume (*right*) in the CA1 SLM, normalized to WT. *VGLUT2*: WT, N = 6, 100.0 ± 9.9 %; KO, N = 5, 146.2 ± 10.9 %. * p = 0.01. *Homer1*: WT, N = 6, 100.0 ± 6.9 %; KO, N = 5, 121.3 ± 11.6 %. p = 0.14. *Co-localized*: WT, N = 6, 100.0 ± 16.8 %; KO, N = 5, 190.3 ± 30.9 %. * p = 0.02. **E** Same as in **C**, but for the DGML. **F** Same as in **D**, applied to the DGML. *VGLUT2*: WT, N = 6, 100.0 ± 9.6 %; KO, N = 5, 142.7 ± 12.6 %. * p = 0.02. *Homer1*: WT, N = 6, 100.0 ± 3.8%; KO, N = 5, 150.7 ± 23.2 %. * p = 0.04. *Co-localized*: WT, N = 6, 100.0 ± 19.1 %; KO, N = 5, 224.1 ± 39.3 %. * p = 0.01. All data for this and subsequent figures are presented as mean ± SEM. Unless stated otherwise, a two-tailed unpaired t-test was used, * p < 0.05, ** p < 0.01.
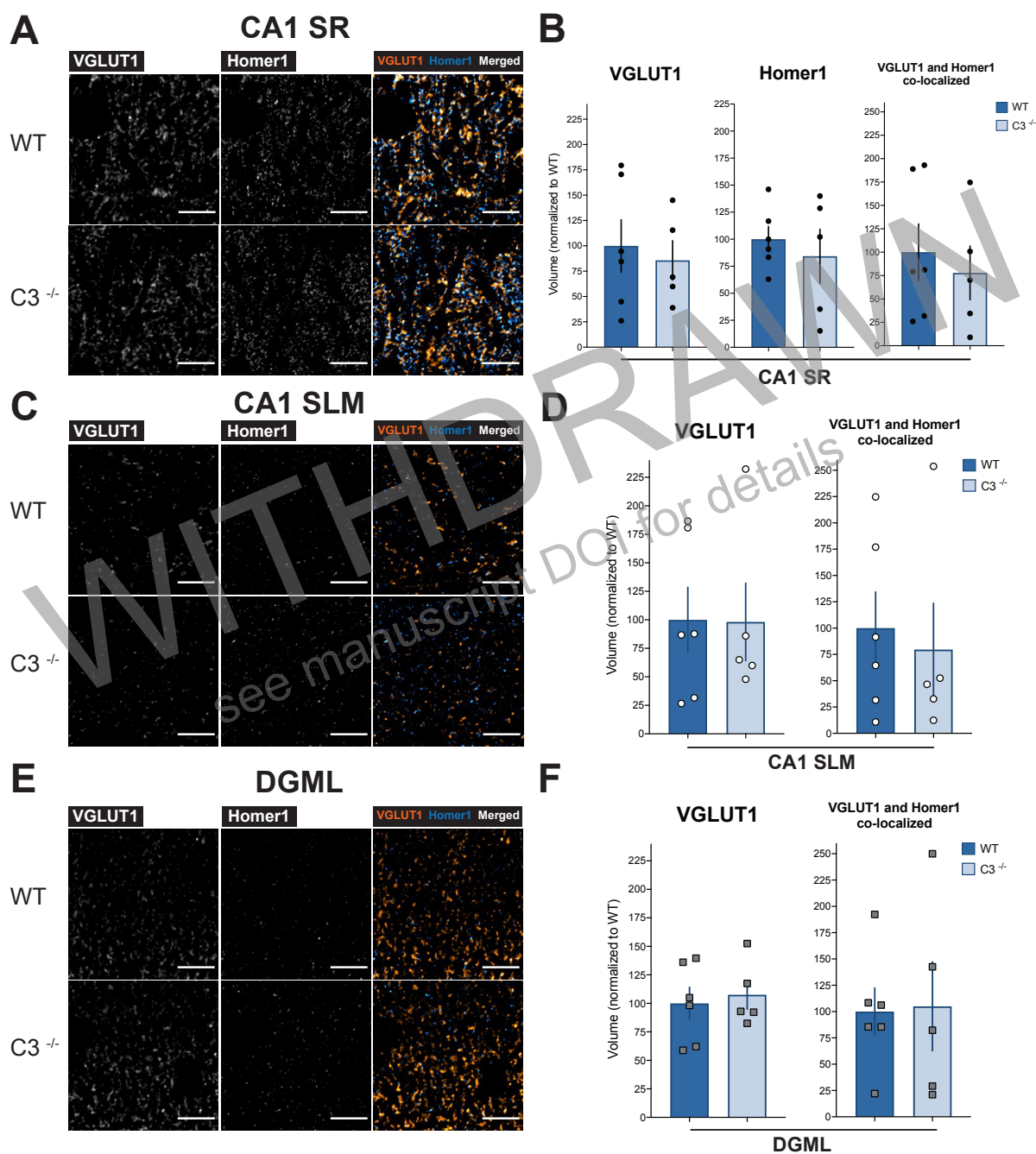
20

Figure 2. *VGLUT1+ synapses are unaffected in C3-/- mice.* **A** Representative single plane

confocal images of VGLUT1, Homer1 and co-localized VGLUT1 and Homer1 in the CA1

SR of WT and C3-/- mice. Scale bars, 10 μm. **B** Quantification of VGLUT1 (*left*), Homer1

(*middle*) and VGLUT1 and Homer1 co-localized volume (*right*) in the CA1 SR, normalized to WT. *VGLUT1*: WT, N = 6, 100.0 ± 25.9 %; KO, N = 5, 85.7 ± 19.4 %. p = 0.68. *Homer1*: WT, N = 6, 100.0 ± 11.7 %; KO, N = 5, 84.3 ± 25.0%. p = 0.56. *Co-localized*: WT, N = 6, 100.0 ± 30.3 %; KO, N = 5, 77.8 ± 28.8 %. p = 0.61. **C** Same as in **A**, but for the CA1 SLM. **D** Quantification of VGLUT1 (*left*) and VGLUT1 and Homer1 co-localized volume (*right*) in the CA1 SLM, normalized to WT. *VGLUT1:* WT, N = 6, 100.0 ± 28.5 %; KO, N = 5, 98.2 ± 34.1 %. p = 0.97. *Co-localized*: WT, N = 6, 100.0 ± 34.4 %; KO, N = 5, 79.6 ± 44.1 %. p = 0.72. **E** Same as in **A, C**, but applied to the DGML. **F** Same as in **D**, but for the DGML. *VGLUT1*: WT, N = 6, 100.0 ± 14.2 %; KO, N = 5, 107.5 ± 12.6 %. p = 0.71. *Co-localized*: WT, N = 6, 100.0 ± 22.5 %; KO, N = 5, 105.0 ± 42.3%. p = 0.91.
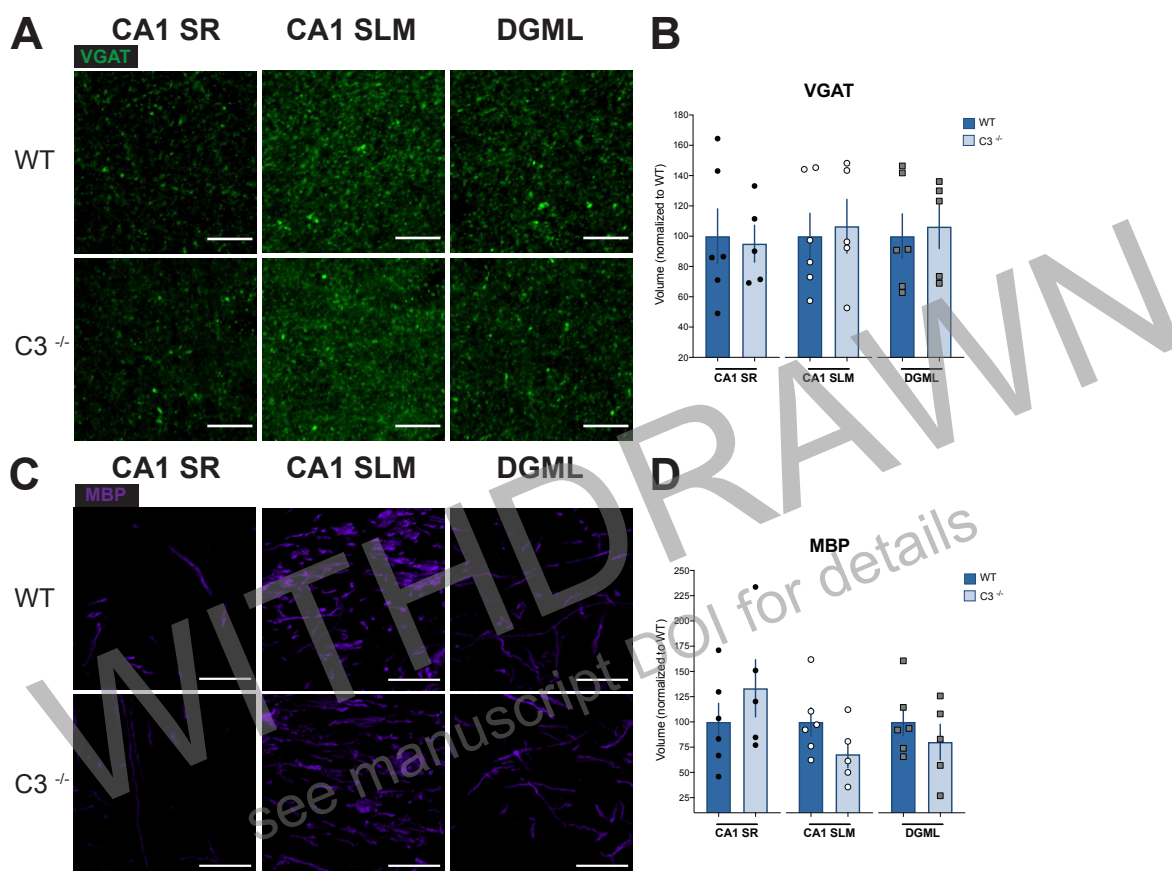
Figure 3. *Inhibitory synapses and myelination are unaltered in C3⁻/⁻ mice.* **A** Representative MIP images of VGAT in the CA1 SR, CA1 SLM and DGML. Scale bars, 10 μm. **B** Quantification of VGAT volume, normalized to WT. *CA1 SR*: WT, N = 6, 100.0 ± 18.1 %; KO, N = 5, 95.1 ± 12.2 %. p = 0.83. *CA1 SLM*: WT, N = 6, 100.0 ± 15.1 %; KO, N = 5, 106.6 ± 17.8 %. p = 0.78. *DGML*: WT, N = 6,100.0 ± 14.8 %; KO, N = 5, 106.3 ± 14.5 %. p = 0.77. **C** Representative MIP images of MBP in the CA1 SR, CA1 SLM and DGML. Scale bars, 20 μm. **D** Quantification of MBP volume, normalized to WT. *CA1 SR*: WT, N = 6, 100.0 ± 18.5 %; KO, N = 5, 133.3 ± 28.4 %. p = 0.34. *CA1 SLM*: WT, N = 6, 100.0 ± 14.1 %; KO, N = 5, 68.0 ± 13.3 %. p = 0.14. *DGML*: WT, N = 6,100.0 ± 14.0 %; KO, N = 5, 80.1 ± 17.7 %. p = 0.39.
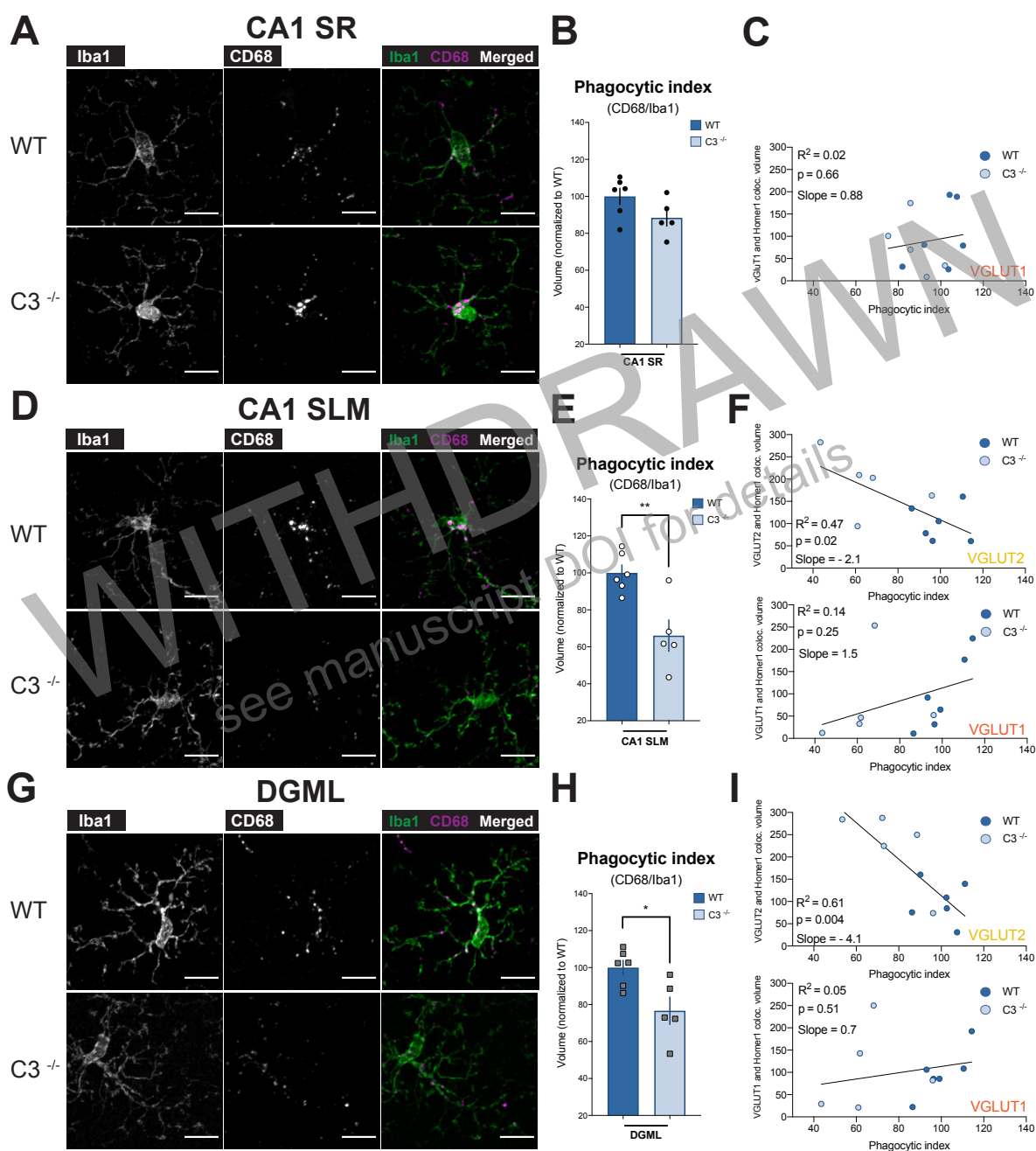
23

Figure 4. *C3^-/- mice have reduced microglial phagocytic activity in VGLUT2^+ regions.* **A**

Representative MIP images of Iba1 and CD68 in the CA1 SR. Scale bars, 10 µm. **B**

Quantification of CD68/Iba1 volume, termed 'phagocytic index', in the CA1 SR,

normalized to WT. WT, N = 6, 100.0 ± 4.4 %; KO, N = 5, 88.4 ± 4.5 %. p = 0.10. **C**

Correlation between VGLUT1 and Homer1 co-localized volume and phagocytic index in

the CA1 SR. Linear regression is shown by the black line. **D** Same as in **A**, but for the

CA1 SLM. **E** Same as in **B**, plotted for the CA1 SLM. WT, N = 6, 100.0 ± 4.3 %; KO, N =

5, 66.1 ± 8.5 %. ** p = 0.005. **F** Correlation between VGLUT2 (*upper*) or VGLUT1 (*lower*)

and Homer1 co-localized volume against phagocytic index in the CA1 SLM of WT and

C3$^{-/-}$ mice. Linear regression is shown by the black line. **G** Same as in **A, D**, but for the

DGML. **H** Same analysis as in **B, E**, but for the DGML. WT, N = 6,100.0 ± 4.0 %; KO, N

= 5, 76.7 ± 7.4 %. * p = 0.02. **I** Same as in **F**, analyzed for the DGML.

25

Acknowledgements

Author contributions

EWS, JG and GLC designed the study and wrote the manuscript. EWS and GL performed data collection and analysis. FJ, LTR and SC provided technical support for IHF and WB experiments. LZ, AK and JW performed the mouse genotyping.

Conflict of interest

The authors have no conflicts of interest to declare.

References

Akers, K.G., Martinez-Canabal, A., Restivo, L., Yiu, A.P., De Cristofaro, A., Hsiang, H.L.L., Wheeler, A.L., Guskjolen, A., Niibori, Y., Shoji, H. et al. (2014). Hippocampal neurogenesis regulates forgetting during adulthood and infancy. Science *344*, 598-602.

Andersen, P., Morris, R., Amaral, D., Bliss, T., and O'Keefe, J. (2006). The hippocampus book. (Oxford University Press).

Basilico, B., Pagani, F., Grimaldi, A., Cortese, B., Di Angelantonio, S., Weinhard, L., Gross, C., Limatola, C., Maggi, L. and Ragozzino, D. (2019). Microglia shape presynaptic properties at developing glutamatergic synapses. Glia *67*, 53-67.

Berry, C.T., Sceniak, M.P., Zhou, L., and Sabo, S.L. (2012). Developmental up-regulation of vesicular glutamate transporter-1 promotes neocortical presynaptic terminal development. PLoS One *7*, e50911.

Bie, B., Wu, J., Foss, J.F., and Naguib, M. (2019). Activation of mGluR1 mediates C1q-dependent microglial phagocytosis of glutamatergic synapses in Alzheimer's rodent models. Molecular neurobiology *56*, 5568-5585.

Boulland, J.L., Qureshi, T., Seal, R.P., Rafiki, A., Gundersen, V., Bergersen, L.H., Fremeau, R.T. Jr., Edwards, R.H., Storm-Mathisen, J. and Chaudhry, F. A. (2004). Expression of the vesicular glutamate transporters during development indicates the widespread corelease of multiple neurotransmitters. Journal of Comparative Neurology *480*, 264-280.

27

Braak, H., Alafuzoff, I., Arzberger, T., Kretzschmar, H., and Del Tredici, K. (2006). Staging of Alzheimer disease-associated neurofibrillary pathology using paraffin sections and immunocytochemistry. Acta neuropathologica *112*, 389-404.

Cheadle, L., Tzeng, C.P., Kalish, B.T., Harmin, D.A., Rivera, S., Ling, E., Nagy, M.A., Hrvatin, S., Hu, L., Stroud, H. et al. (2018). Visual experience-dependent expression of Fn14 is required for retinogeniculate refinement. Neuron *99*, 525-539.

Chung, W.S., Welsh, C.A., Barres, B.A., and Stevens, B. (2015). Do glia drive synaptic and cognitive impairment in disease?. Nature neuroscience *18*, 1539-1545.

Comer, A.L., Jinadasa, T., Sriram, B., Phadke, R. A., Kretsge, L. N., Nguyen, T. P., Antognetti, G., Gilbert, J.P., Lee, J., Newark, E.R. et al. (2020). Increased expression of schizophrenia-associated gene C4 leads to hypoconnectivity of prefrontal cortex and reduced social interaction. PLoS Biology *18*, e3000604.

Davalos, D., Grutzendler, J., Yang, G., Kim, J.V., Zuo, Y., Jung, S., Littman, D.R., Dustin, M.L. and Gan, W. B. (2005). ATP mediates rapid microglial response to local brain injury in vivo. Nature neuroscience *8*, 752-758.

Dejanovic, B., Huntley, M.A., De Mazière, A., Meilandt, W.J., Wu, T., Srinivasan, K., Jiang, Z., Gandham, V., Friedman, B.A., Ngu, H. et al. (2018). Changes in the synaptic

proteome in tauopathy and rescue of tau-induced synapse loss by C1q antibodies. Neuron *100*, 1322-1336.

Dissing-Olesen, L., LeDue, J.M., Rungta, R.L., Hefendehl, J.K., Choi, H.B., & MacVicar, B.A. (2014). Activation of neuronal NMDA receptors triggers transient ATP-mediated microglial process outgrowth. Journal of Neuroscience *34*, 10511-10527.

Eyo, U.B., Bispo, A., Liu, J., Sabu, S., Wu, R., DiBona, V.L., Zheng, J., Tang, Y. et al. (2018). The GluN2A subunit regulates neuronal NMDA receptor-induced microglia-neuron physical interactions. Scientific Reports *8*, 1-10.

Filipello, F., Morini, R., Corradini, I., Zerbi, V., Canzi, A., Michalski, B., Erreni, M., Markicevic, M., Starvaggi-Cucuzza C., Otero, K. et al. (2018). The microglial innate immune receptor TREM2 is required for synapse elimination and normal brain connectivity. Immunity *48*, 979-991.

Fonseca, M.I., Chu, S.H., Hernandez, M.X., Fang, M.J., Modarresi, L., Selvan, P., Macgregor, G.R. and Tenner, A.J. (2017). Cell-specific deletion of C1qa identifies microglia as the dominant source of C1q in mouse brain. Journal of neuroinflammation *14*, 48.

Fremeau R.T. Jr., Troyer, M.D., Pahner, I., Nygaard, G.O., Tran, C.H., Reimer, R.J., Bellocchio, E.E., Fortin, D., Storm-Mathisen, J. and Edwards, R.H. (2001). The

29

expression of vesicular glutamate transporters defines two classes of excitatory synapse. Neuron *31*, 247-260.

Fremeau, R.T. Jr., Kam, K., Qureshi, T., Johnson, J., Copenhagen, D.R., Storm-Mathisen, J., Chaudhry, F.A., Nicoll, R.A. and Edwards, R.H. (2004). Vesicular glutamate transporters 1 and 2 target to functionally distinct synaptic release sites. Science *304*, 1815-1819.

Ginhoux, F., Greter, M., Leboeuf, M., Nandi, S., See, P., Gokhan, S., Mehler, M.F., Conway, S.J., Ng, L.G., Stanley, E.R. et al. (2010). Fate mapping analysis reveals that adult microglia derive from primitive macrophages. Science *330*, 841-845.

Gómez-Isla, T., Price, J.L., McKeel , D.W. Jr., Morris, J.C., Growdon, J.H., and Hyman, B.T. (1996). Profound loss of layer II entorhinal cortex neurons occurs in very mild Alzheimer's disease. Journal of Neuroscience *16*, 4491-4500.

Guskjolen, A., Kenney, J.W., de la Parra, J., Yeung, B.R.A., Josselyn, S. A., and Frankland, P.W. (2018). Recovery of "lost" infant memories in mice. Current Biology *28*, 2283-2290.

Györffy, B.A., Kun, J., Török, G., Bulyáki, É., Borhegyi, Z., Gulyássy, P., Kis, V., Szocsics, P., Micsonai, A., Matkó, J. et al. (2018). Local apoptotic-like mechanisms

underlie complement-mediated synaptic pruning. Proceedings of the National Academy of Sciences *115*, 6303-6308.

Hagemeyer, N., Hanft, K.M., Akriditou, M.A., Unger, N., Park, E.S., Stanley, E.R., Staszewski, O., Dimou, L. and Prinz, M. (2017). Microglia contribute to normal myelinogenesis and to oligodendrocyte progenitor maintenance during adulthood. Acta neuropathologica *134*, 441-458.

Hallett, P.J., Collins, T.L., Standaert, D.G., and Dunah, A.W. (2008). Biochemical fractionation of brain tissue for studies of receptor distribution and trafficking. Current protocols in neuroscience *42*, 1-16.

Hammond, J. W., Bellizzi, M.J., Ware, C., Qiu, W.Q., Saminathan, P., Li, H., Luo, S., Ma, S.A., Li, Y. and Gelbard, H. A. (2020). Complement-dependent synapse loss and microgliosis in a mouse model of multiple sclerosis. Brain, Behavior, and Immunity, 10.1016/j.bbi.2020.03.004.

Hong, S., Beja-Glasser, V.F., Nfonoyim, B.M., Frouin, A., Li, S., Ramakrishnan, S., Merry, K.M., Shi, Q., Rosenthal, A., Barres, B.A. et al. (2016). Complement and microglia mediate early synapse loss in Alzheimer mouse models. Science *352*, 712-716.

Hua, J.Y., and Smith, S.J. (2004). Neural activity and the dynamics of central nervous system development. Nature Neuroscience *7*, 327-332.

Hughes, A.N. and Appel, B. (2019). Developmental myelination is modified by microglial pruning. bioRxiv, 659482.

Huijbers, W., Mormino, E.C., Wigman, S.E., Ward, A.M., Vannini, P., McLaren, D.G., Becker, J.A., Schultz, A.P., Hedden, T., Johnson, K.A. et al. (2014). Amyloid deposition is linked to aberrant entorhinal activity among cognitively normal older adults. Journal of Neuroscience *34*, 5200-5210.

Huttenlocher, P.R. (1979). Synaptic density in human frontal cortex-developmental changes and effects of aging. Brain Res. *163*, 195-205.

Katz, L.C., and Shatz, C.J. (1996). Synaptic activity and the construction of cortical circuits. Science *274*, 1133-1138.

Khan, U.A., Liu, L., Provenzano, F.A., Berman, D.E., Profaci, C.P., Sloan, R., Mayeux, R., Duff, K.E. and Small, S.A. (2014). Molecular drivers and cortical spread of lateral entorhinal cortex dysfunction in preclinical Alzheimer's disease. Nature Neuroscience *17*, 304-311.

Kim, D.D., and Song, W.C. (2006). Membrane complement regulatory proteins. Clinical Immunology *118*, 127-136.

Kopec, A.M., Smith, C.J., Ayre, N.R., Sweat, S.C., and Bilbo, S.D. (2018). Microglial dopamine receptor elimination defines sex-specific nucleus accumbens development and social behavior in adolescent rats. *Nature Communications 9*, 1-16.

Lehmann, K.S., Wood, A., Cummings, D., Bai, L., Stevens, B. and Belluscio, L. (2018). Complement 3 signaling is necessary for the developmental refinement of olfactory bulb circuitry. bioRxiv, 449454.

Lehrman, E.K., Wilton, D.K., Litvina, E.Y., Welsh, C.A., Chang, S.T., Frouin, A., Walker, A.J., Heller, M.D., Umemori, H., Chen, C. et al. (2018). CD47 protects synapses from excess microglia-mediated pruning during development. Neuron *100*, 120-134.

Li, Q., Cheng, Z., Zhou, L., Darmanis, S., Neff, N.F., Okamoto, J., Gulati, G., Bennett, M.L., Sun, L.O., Clarke, L.E. et al. (2019). Developmental heterogeneity of microglia and brain myeloid cells revealed by deep single-cell RNA sequencing. Neuron *101*, 207-223.

Li, T., Chiou, B., Gilman, C.K., Luo, R., Koshi, T., Yu, D., Oak, H.C., Giera, S., Johnson-Venkatesh, E., Muthukumar, A.K. et al. (2020). A splicing isoform of GPR56 mediates microglial synaptic refinement via phosphatidylserine binding. bioRxiv. https://doi.org/10.1101/2020.04.24.059840

33

Litvinchuk, A., Wan, Y.W., Swartzlander, D.B., Chen, F., Cole, A., Propson, N.E., Wang, Q., Zhang, B., Liu, Z. and Zheng, H. (2018). Complement C3aR inactivation attenuates tau pathology and reverses an immune network deregulated in tauopathy models and Alzheimer's disease. Neuron *6*, 1337-1353.

Liu, Y.U., Ying, Y., Li, Y., Eyo, U.B., Chen, T., Zheng, J., Umpierre, A.D., Zhu, J., Bosco, D.B., Dong, H. et al. (2019). Neuronal network activity controls microglial process surveillance in awake mice via norepinephrine signaling. Nature Neuroscience *11*, 1771-1781.

Lui, H., Zhang, J., Makinson, S.R., Cahill, M.K., Kelley, K.W., Huang, H.Y., Shang, Y., Oldham, M.C., Martens, L.H., Gao, F. et al. Progranulin deficiency promotes circuit-specific synaptic pruning by microglia via complement activation. Cell *165*, 921-935.

Nimmerjahn, A., Kirchhoff, F., and Helmchen, F. (2005). Resting microglial cells are highly dynamic surveillants of brain parenchyma in vivo. Science *308*, 1314-1318.

Paolicelli, R.C., Bolasco, G., Pagani, F., Maggi, L., Scianni, M., Panzanelli, P., Giustetto, M., Ferreira, T.A., Guiducci, E., Dumas, L. et al. (2011). Synaptic pruning by microglia is necessary for normal brain development. Science *333*, 1456-1458.

Park J., Jung, E., Lee, S.H., Chung, W.S. (2020) CDC50A dependent phosphatidylserine exposure induces inhibitory post- synapse elimination by microglia. bioRxiv. https://doi.org/10.1101/2020.04.25.060616.

Perdiguero, E.G., Klapproth, K., Schulz, C., Busch, K., Azzoni, E., Crozet, L., Garner, H., Trouillet, C., de Brujin, M.F., Geissmann, F. et al. (2015). Tissue-resident macrophages originate from yolk-sac-derived erythro-myeloid progenitors. Nature *518*, 547-551.

Perez-Alcazar, M., Daborg, J., Stokowska, A., Wasling, P., Björefeldt, A., Kalm, M., Zetterberg, H., Carlström, K.E., Blomgren, K., Ekdahl, C.T. et al. (2014). Altered cognitive performance and synaptic function in the hippocampus of mice lacking C3. Experimental Neurology *253*, 154-164.

Petanjek, Z., Judaš, M., Šimić, G., Rašin, M. R., Uylings, H. B., Rakic, P., and Kostović, I. (2011). Extraordinary neoteny of synaptic spines in the human prefrontal cortex. Proceedings of the National Academy of Sciences *108*, 13281-13286.

Ricklin, D., Hajishengallis, G., Yang, K., and Lambris, J.D. (2010). Complement: a key system for immune surveillance and homeostasis. Nature Immunology *11*, 785-797.

Roy, E.R., Wang, B., Wan, Y.W., Chiu, G.S., Cole, A.L., Yin, Z., Propson, N.E., Xu, Y., Jankowsky, J.L., Liu Z. et al. (2020). Type I interferon response drives neuroinflammation and synapse loss in Alzheimer disease. The Journal of Clinical Investigation *130*, 1912-1930.

35

Salter, M. W., and Stevens, B. (2017). Microglia emerge as central players in brain disease. Nature Medicine *23*, 1018-1027.

Schafer, D.P., Lehrman, E.K., Kautzman, A.G., Koyama, R., Mardinly, A.R., Yamasaki, R., Ransohoff, R.M., Greenberg, M.E., Barres, B.A. and Stevens, B. (2012). Microglia sculpt postnatal neural circuits in an activity and complement-dependent manner. Neuron *74*, 691-705.

Schafer, D.P., Lehrman, E.K., Heller, C T., and Stevens, B. (2014). An engulfment assay: a protocol to assess interactions between CNS phagocytes and neurons. JoVE (Journal of Visualized Experiments) *88*, 10.3791/51482.

Scott-Hewitt, N.J., Perrucci, F., Morini, R., Erreni, M., Mahoney, M., Witkowska, A., Carey, A., Faggiani, E., Theresia Schuetz, L., Mason, S. et al. (2020). Local externalization of phosphatidylserine mediates developmental synaptic pruning by microglia. bioRxiv, https://doi.org/10.1101/2020.04.24.059584

Sekar, A., Bialas, A.R., de Rivera, H., Davis, A., Hammond, T.R., Kamitaki, N., Tooley, K., Presumey, J., Baum, M., Van Doren, V. et al. (2016). Schizophrenia risk from complex variation of complement component 4. Nature *530*, 177-183.

Sellgren, C.M., Gracias, J., Watmuff, B., Biag, J.D., Thanos, J.M., Whittredge, P.B., Fu, T., Worringer, K., Brown, H.E., Wang, J. et al. (2019). Increased synapse

elimination by microglia in schizophrenia patient-derived models of synaptic pruning. Nature Neuroscience *22*, 374-385.

Sheng, M., and Kim, E. (2011). The postsynaptic organization of synapses. Cold Spring Harbor Perspectives in Biology *3*, a005678.

Shi, Q., Colodner, K.J., Matousek, S.B., Merry, K., Hong, S., Kenison, J.E., Frost, J.L., Le, K.X., Li, S., Dodart, J.C. et al. (2015). Complement C3-deficient mice fail to display age-related hippocampal decline. Journal of Neuroscience *35*, 13029-13042.

Shi, Q., Chowdhury, S., Ma, R., Le, K.X., Hong, S., Caldarone, B.J., Stevens, B. and Lemere, C.A. (2017). Complement C3 deficiency protects against neurodegeneration in aged plaque-rich APP/PS1 mice. Science Translational Medicine *9*, eaaf6295.

Small, S. A., Schobel, S.A., Buxton, R.B., Witter, M.P., and Barnes, C.A. (2011). A pathophysiological framework of hippocampal dysfunction in ageing and disease. Nature Reviews Neuroscience *12*, 585-601.

Stephan, A.H., Barres, B A., and Stevens, B. (2012). The complement system: an unexpected role in synaptic pruning during development and disease. Annual Review of Neuroscience *35*, 369-389.

37

Stephan, A.H., Madison, D.V., Mateos, J.M., Fraser, D.A., Lovelett, E.A., Coutellier, L., Kim, L., Tsai, H.H., Huang, E.J. Rowitch, D.H. et al. (2013). A dramatic increase of C1q protein in the CNS during normal aging. The Journal of Neuroscience *33*, 13460-13474.

Stevens, B., Allen, N.J., Vazquez, L.E., Howell, G.R., Christopherson, K.S., Nouri, N., Micheva, K.D., Mehalow, A.K., Huberman, A.D., Stafford, B. et al. (2007). The classical complement cascade mediates CNS synapse elimination. Cell *131*, 1164-1178.

Thal, D.R., Rüb, U., Orantes, M., and Braak, H. (2002). Phases of Aβ-deposition in the human brain and its relevance for the development of AD. Neurology *58*, 1791-1800.

Vasek, M.J., Garber, C., Dorsey, D., Durrant, D.M., Bollman, B., Soung, A., Yu, J., Perez-Torres, C., Frouin, A., Wilton, D.K. et al. (2016). A complement-microglial axis drives synapse loss during virus-induced memory impairment. Nature *534*, 538-543.

Vukojicic, A., Delestree, N., Fletcher., E.V., Pagiazitis, J.G., Sankaranarayanan, S., Yednock, T.A., Barres, B.A., Mentis, G.Z. (2019). The classical complement pathway mediates microglia-dependent remodeling of spinal motor circuits during development and in SMA. Cell Reports *29*, 3087-3100.

Wang, C., Yue, H., Hu, Z., Shen, Y., Ma, J., Li, J., Wang, X.D., Wang, L., Sun, B., Shi, P. et al. (2020). Microglia mediate forgetting via complement-dependent synaptic elimination. Science *367*, 688-694.

Wang, Y., Cella, M., Mallinson, K., Ulrich, J.D., Young, K.L., Robinette, M.L., Gilfillan, S., Krishnan, G.M., Sudhakar, S., Zinselmeyer, B.H. et al. (2015). TREM2 lipid sensing sustains the microglial response in an Alzheimer's disease model. Cell *160*, 1061-1071.

Watkins, L.M., Neal, J.W., Loveless, S., Michailidou, I., Ramaglia, V., Rees, M.I., Reynolds, R., Robertson, N.P., Morgan, B.P. and Howell, O.W. (2016). Complement is activated in progressive multiple sclerosis cortical grey matter lesions. Journal of Neuroinflammation *13*, 10.1186/s12974-016-0611-x.

Weinhard, L., di Bartolomei, G., Bolasco, G., Machado, P., Schieber, N.L., Neniskyte, U., Exiga, M., Vadisiute, A., Raggioli, A. Schertel, A. et al. (2018). Microglia remodel synapses by presynaptic trogocytosis and spine head filopodia induction. Nature Communications *9*, 10.1038/s41467-018-03566-5.

Werneburg, S., Jung, J., Kunjamma, R.B., Ha, S.K., Luciano, N.J., Willis, C M., Gao, G., Biscola, N.P., Havton, L.A., Crocker, S.J. et al. (2020). Targeted complement inhibition at synapses prevents microglial synaptic engulfment and synapse loss in demyelinating disease. Immunity *52*, 167-182.

Wessels, M. R., Butko, P., Ma, M., Warren, H.B., Lage, A.L., and Carroll, M.C. (1995). Studies of group B streptococcal infection in mice deficient in complement component C3 or C4 demonstrate an essential role for complement in both innate and acquired immunity. Proceedings of the National Academy of Sciences *92*, 11490-11494.

Wouterlood, F.G., Aliane, V., Boekel, A.J., Hur, E E., Zaborszky, L., Barroso-Chinea, P., Härtig, W., Lanciego, J.L. and Witter, M.P. (2008). Origin of calretinin-containing, vesicular glutamate transporter 2-coexpressing fiber terminals in the entorhinal cortex of the rat. Journal of Comparative Neurology *506*, 359-370.

Wu, T., Dejanovic, B., Gandham, V. D., Gogineni, A., Edmonds, R., Schauer, S., Srinivasan, K., Huntley, M.A., Wang, Y. Wang, T.M. et al. (2019). Complement C3 is activated in human AD brain and is required for neurodegeneration in mouse models of amyloidosis and tauopathy. Cell Reports *28*, 2111-2123.

Yang, X., Yao, C., Tian, T., Li, X., Yan, H., Wu, J., Li, H., Pei, L., Liu, D., Tian, Q. et al. (2018). A novel mechanism of memory loss in Alzheimer's disease mice via the degeneration of entorhinal–CA1 synapses. Molecular Psychiatry *23*, 199-210.

Yekhlef, L., Breschi, G.L., and Taverna, S. (2017). Optogenetic activation of VGLUT2-expressing excitatory neurons blocks epileptic seizure-like activity in the mouse entorhinal cortex. Scientific Reports *7*, 10.1038/srep43230.

Zhang, J., Malik, A., Choi, H.B., Ko, R.W., Dissing-Olesen, L., and MacVicar, B.A. (2014). Microglial CR3 activation triggers long-term synaptic depression in the hippocampus via NADPH oxidase. Neuron *82*, 195-207.

Zhong, S., Ding, W., Sun, L., Lu, Y., Dong, H., Fan, X., Liu, Z., Chen, R., Zhang, S., Ma, Q. et al. (2020). Decoding the development of the human hippocampus. Nature *577*, 531-536.